J. Cent. South Univ. (2012) 19: 1497−1502
DOI: 10.1007/s11771-012-1167-2

Springer

Influence of Yb_2O_3 doping on microstructural and electrical properties of ZnO−Bi_2O_3-based varistor ceramics

XU Dong(徐东)[1, 2, 3, 4], TANG Dong-mei(唐冬梅)[1, 5], LIN Yuan-hua(林元华)[6],
JIAO Lei(焦雷)[1], ZHAO Guo-ping(赵国平)[1], CHENG Xiao-nong(程晓农)[1, 5]

1. State Key Laboratory of Power Transmission Equipment & System Security and New Technology (College of Electrical Engineering, Chongqing University), Chongqing 400044, China;
2. School of Materials Science and Engineering, Jiangsu University, Zhenjiang 212013, China;
3. Key Laboratory of Semiconductor Materials Science (Institute of Semiconductors, Chinese Academy of Sciences), Beijing 100083, China;
4. State Key Laboratory of Electrical Insulation and Power Equipment (Xi'an Jiaotong University), Xi'an 710049, China;
5. Changzhou Engineering Research Institute of Jiangsu University, Changzhou 213000, China;
6. State Key Laboratory of New Ceramic and Fine Processing (Tsinghua University), Beijing 100083, China

Abstract: ZnO−Bi_2O_3-based varistor ceramics doped with Yb_2O_3 in the range from 0 to 0.4% (molar fraction) were obtained by a solid reaction route. The X-ray diffractometry (XRD) and scanning electron microscopy (SEM) were applied to characterize the phases and microstructure of the varistor ceramics, and a DC parameter instrument for varistor ceramics was applied to investigate their electrical properties and *V*−*I* characteristics. The XRD analysis of the samples shows that the ZnO phase, Bi_2O_3 phase, $Zn_7Sb_2O_{12}$-type spinel phase and $Zn_2Bi_3Sb_3O_{14}$-type pyrochlore are present, and the Yb_2O_3 phases and Sb_2O_4 phases are found in varistor ceramics with increasing amounts of Yb_2O_3. The average size of ZnO grain firstly increases and then decreases with the increase of Yb_2O_3 content. The result also shows that the threshold voltage is between 656 V/mm and 1 232 V/mm, the nonlinear coefficient is in the range of 14.1−22.3, and the leakage current is between 0.60 μA and 19.6 μA. The 0.20% Yb_2O_3-added ZnO−Bi_2O_3-based varistor ceramics sintered at 900 °C have the best electrical characteristics.

Key words: varistor ceramics; zinc oxide; Yb_2O_3; microstructure; electrical properties

1 Introduction

ZnO varistor ceramics are polycrystalline semiconducting ceramics that are widely used as voltage stabilization and surge arresters in electric power systems [1−5]. These varistors have highly nonlinear voltage (*V*)−current (*I*) characteristics, often expressed by $I=KV^{\alpha}$, where *K* is a constant and α is nonlinear exponent. This appearance is due to the presence of a double Schottky barrier (DSB) formed at grain boundaries [6−8]. The current density–electric field (*J*–*E*) characteristics of ZnO varistor ceramics are expressed by the following empirical equation: $J=K'E^{\alpha'}$ where K' is a constant and α' is the nonlinear coefficient. Commercial varistors are usually made by solid state ZnO particles with doping agent oxides such as Bi_2O_3, Sb_2O_3, Co_2O_3, MnO_2 and Cr_2O_3, and the mixed powders then are pressed and sintered at higher temperatures to produce the dense, final products. The microstructure of the sintered material comprises a matrix of highly conductive ZnO grains with two major secondary phases: a spinel type phase mainly located at the grain boundaries and triple points, and a Bi-rich phase surrounding the ZnO grains and promoting the formation of potential barriers to electrical conduction at the ZnO homojunctions. As the varistors possess the nonlinear electrical behavior, an ideal varistor should only consist of homogeneously distributed ZnO grains with highly resistive grain boundaries and without secondary phases. To achieve a high breakdown voltage, changing the varistor thickness or decreasing the average size of the ZnO grains is useful

Foundation item: Project(BK2011243) supported by the Natural Science Foundation of Jiangsu Province, China; Project(2007DA10512711408) supported by the Visiting Scholarship of State Key Laboratory of Power Transmission Equipment & System Security and New Technology (Chongqing University), China; Project(EIPE11204) supported by the State Key Laboratory of Electrical Insulation and Power Equipment, China; Project(KF201104) supported by the State Key Laboratory of New Ceramic and Fine Processing, China; Project(KFJJ201105) supported by the Opening Project of State Key Laboratory of Electronic Thin Films and Integrated Devices, China; Project(10KJD430002) supported by the Universities Natural Science Research Project of Jiangsu Province, China; Project(11JDG084) supported by the Research Foundation of Jiangsu University, China
Received date: 2011−06−02; **Accepted date:** 2011−09−18
Corresponding author: XU Dong, PhD; Tel: +86−511−88797633; E-mail: frank@ujs.edu.cn

to increase the number of barriers or grain boundaries [6]. ASHRAF et al [6] and HOUABES and METZ [9] revealed that addition of rare-earth oxides in the starting composition decreases the average grain size, and many researches [5, 9−14] investigated the influence of different rare earth oxides, such as Y_2O_3, Sc_2O_3, Er_2O_3, Lu_2O_3 and Dy_2O_3 on the microstructure and electrical properties of the ZnO−Bi_2O_3-based varistor ceramics. These investigations show that the rare earth oxides may play an important role in controlling different operation parameters of these kinds of varistor ceramics, and the rare earth oxides may significantly increase the breakdown field.

In this work, the electrical characteristics of the ZnO−Bi_2O_3-based varistor ceramics with different Yb_2O_3 contents are investigated and the results are analyzed. The major aim of this work is to study the influence of the Yb_2O_3 on the microstructures and electrical characteristics of ZnO−Bi_2O_3-based varistor ceramics doped with Yb_2O_3.

2 Experimental

Reagent-grade raw materials with the composition of (96.5−x)% ZnO + 0.7% Bi_2O_3 + 1.0% Sb_2O_3 + 0.8% Co_2O_3 + 0.5% MnO_2 + 0.5% Cr_2O_3 + x% Yb_2O_3 (x = 0, 0.1, 0.2, 0.3 and 0.4, molar fraction, labeled with P0, P1, P2, P3 and P4, respectively) were used to prepare ZnO−Bi_2O_3-based varistor ceramics. The powder mixture was ball-milled using agate ball for 5 h, and then the mixture was dried and sieved by 63 μm screen. The powder was pulverized using an agate mortar/pestle and 2% (mass fraction) polyvinyl alcohol (PVA) was added as binder. The materials were granulated by 150 μm screen to produce starting powder, and the powder was pressed into discs of 12.0 mm in diameter and 2.0 mm in thickness. The discs were sintered at 900, 950 and 1 000 °C for 2 h with a heating rate of 5 °C/min, furnace cooled and then marked with the letters A, B and C, respectively. The sintered samples were lapped and polished to 1.0 mm. The final samples were about 10 mm in diameter and 1.0 mm in thickness. The bulk density (D) of the samples was measured in terms of mass and volume. For the characterization of DC current−voltage, silver pastes were coated and toasted on both sides of the sintered samples, and the ohmic contact of electrodes was formed by heating at 600 °C for 10 min. The diameter of the electrodes was 5 mm.

A V−I source/measure unit (CJP CJ1001) was used to measure varistor voltages (V_N) at 0.1 and 1.0 mA and the threshold voltage V_T (V_T=V_N/d; d is the thickness of the sample). The leakage current (I_L) was measured at 0.75V_N. The nonlinear coefficient is calculated as $\alpha = 1/\lg(V_{1.0mA}/V_{0.1mA})$ [14−17]. The microstructure of samples was analyzed using a scanning electron microscope (SEM, JEOL JSM-7001F) and the phase structure was identified by X-ray diffractometer (XRD, Rigaku D/max 2500, Japan) [14, 18].

3 Results and discussion

XRD patterns of ZnO−Bi_2O_3-based varistor ceramics doped with different amounts of Yb_2O_3 sintered at 900 °C are shown in Fig. 1. In the sample without Yb_2O_3, the phases were identified as ZnO phase, Bi_2O_3 phase, $Zn_7Sb_2O_{12}$-type spinel phase and $Zn_2Bi_3Sb_3O_{14}$-type pyrochlore. However, in samples doped with Yb_2O_3, additional peaks are evident and their intensity increases with the increase of Yb_2O_3 content in the starting composition. In other words, the Yb_2O_3 phases and the Sb_2O_4 phases are found in ZnO−Bi_2O_3-based varistor ceramics with the increase of Yb_2O_3 content.

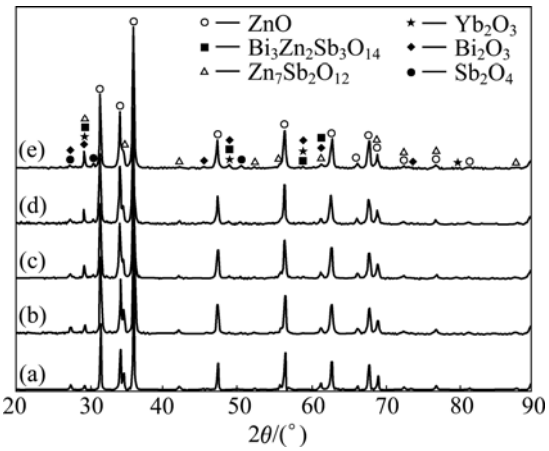

Fig. 1 XRD patterns of ZnO−Bi_2O_3-based varistor ceramics doped with different amounts of Yb_2O_3 sintered at 900 °C: (a) P0A; (b) P1A; (c) P2A; (d) P3A; (e) P4A

Differential thermal and high temperature X-ray analysis have recently suggested the following reactions for the microstructure development of ZnO−Bi_2O_3-based varistor ceramics during reactive liquid phase sintering in the temperature range of 500−1 050 °C [16, 19−20]:

$$Sb_2O_3(s)+O_2 \longrightarrow Sb_2O_5(l)\ (527\ ^\circ C) \quad (1)$$

$$Sb_2O_5(l)+ZnO(s) \longrightarrow ZnSb_2O_6(s)\ (700-800\ ^\circ C) \quad (2)$$

$$ZnSb_2O_6(s)+6ZnO(s) \longrightarrow Zn_7Sb_2O_{12}(s)\ (>800\ ^\circ C) \quad (3)$$

$$3ZnSb_2O_6(s)+3Bi_2O_3(s)+ZnO(s) \longrightarrow 2Zn_2Bi_3Sb_3O_{14}(s)\ (700-900\ ^\circ C) \quad (4)$$

$$2Zn_2Bi_3Sb_3O_{14}(s)+17ZnO(s) \longrightarrow 3Zn_7Sb_2O_{12}(s)+3Bi_2O_3(l)\ (950-1\ 050\ ^\circ C) \quad (5)$$

According to reactions (1)−(4), at the first stage of sintering, after the formation of spinel ($ZnSb_2O_6$, $Zn_7Sb_2O_{12}$) and pyrochlore ($Zn_2Bi_3Sb_3O_{14}$) phases, pyrochlore reacts with ZnO to lead to the appearance of a

liquid bismuth oxide phase by reaction (5), and the formation of spinel is accompanied with the formation of Bi_2O_3 liquid simultaneously. In other words, this liquid oxide might dissolve adjacent solid ZnO phases and generate an eutectic liquid rich in bismuth, and at the same time, the amount of the pyrochlore decreases and that of the spinel increases [19]. The generation of the Bi_2O_3-rich liquid induces the formation of capillary forces, which brings the second phase together to form cluster. As soon as the Bi_2O_3-rich liquid is formed, the vaporization starts. The mass loss of the varistor ceramics thus jumps as the temperature is raised above 1 000 °C [21]. BERNIK et al [22] reported that for the Y_2O_3-doped ZnO−Bi_2O_3-based varistor ceramics, the addition of Y_2O_3 results in the formation of a fine-grained Bi−Zn−Sb−Y−O phase along the grain boundaries of the ZnO grains that inhibits the grain growth. The Y_2O_3-containing phase bounds the Bi_2O_3 and influences the sintering of the samples. Our previously researches [12−13, 23] indicated that doping with rare earth oxides would affect the formation and decomposition of the $Bi_3Zn_2Sb_3O_{14}$ pyrochlore, which promotes the generation of the new phases. In the meantime, doping with rare earth oxides would affect the time that the varistor ceramics spend in the liquid phase, and as this process becomes longer, the vaporization of Bi_2O_3 from the ZnO−Bi_2O_3-based varistor ceramics becomes more serious.

SEM micrographs of fracture surfaces of varistor ceramics doped with different amounts of Yb_2O_3 sintered at 900 °C are shown in Fig. 2. When the content of Yb_2O_3 dopant increases from 0 to 0.2% (molar fraction), the average size of ZnO grain is increased; when the content of Yb_2O_3 is more than 0.2%, the average size of ZnO grain is decreased. When the content of Yb_2O_3 is less than 0.2%, although Yb^{+3} ions have larger radius (0.086 nm) than Zn^{+2} ions (0.074 nm), it is possible that the limited substitution occurs within the ZnO grains by preparing the varistor ceramics using high energy ball milling. Yb substitutes Zn and creates lattice defect in ZnO grains. The chemical defect reaction can be written by Kroger-Vink notation:

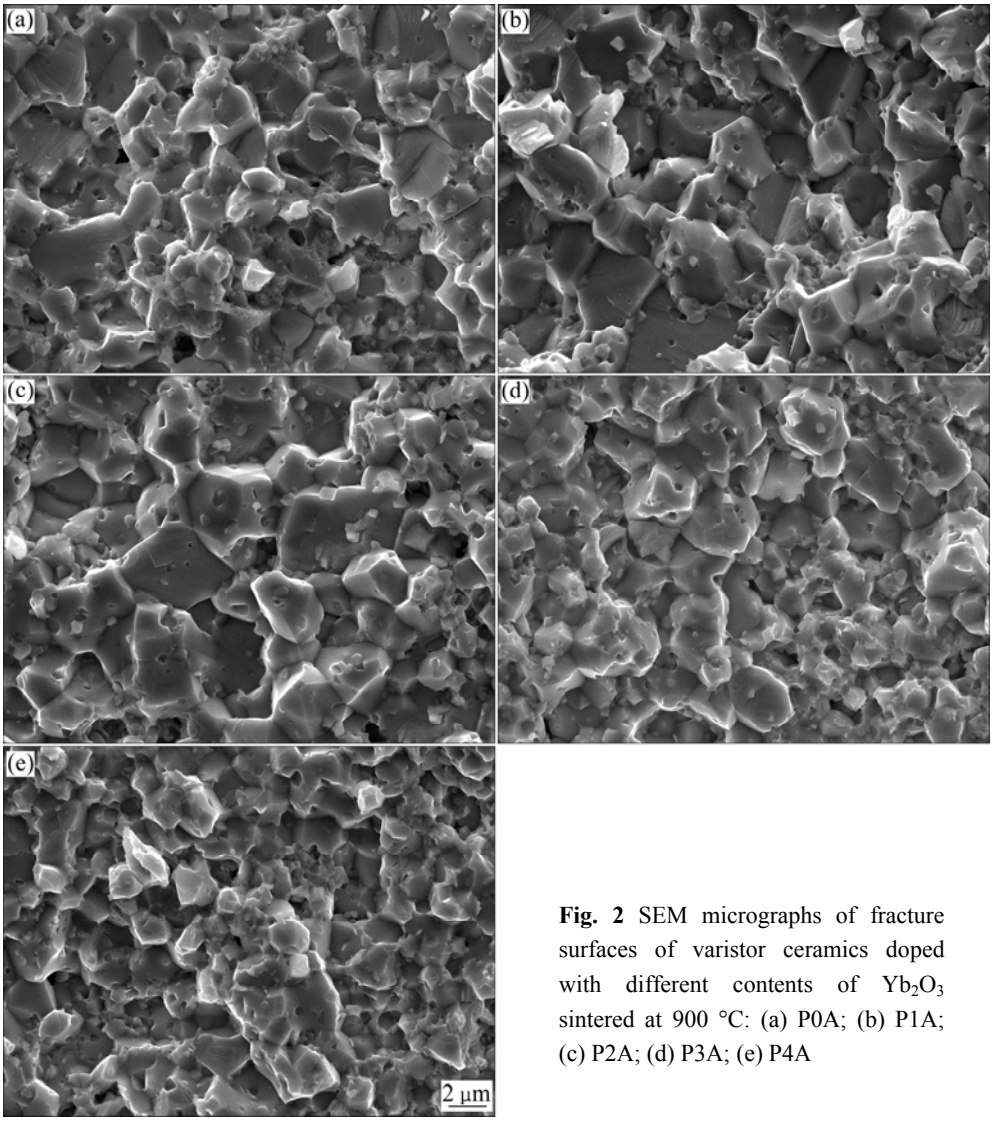

Fig. 2 SEM micrographs of fracture surfaces of varistor ceramics doped with different contents of Yb_2O_3 sintered at 900 °C: (a) P0A; (b) P1A; (c) P2A; (d) P3A; (e) P4A

$$Yb_2O_3 \xrightarrow{ZnO} 2Yb_{Zn}^{g} + V_{Zn}'' + 2O_O^X + 1/2O_2 \quad (6)$$

where Yb_{Zn}^{g} is a positively charged Yb ion substituting Zn lattice site; V_{Zn}'' is a negatively charged Zn vacancy, and O_O^X is a neutral oxygen of oxygen lattice site [24]. At the same time, the little doping with Yb_2O_3 would also affect the formation and decomposition of the $Bi_3Zn_2Sb_3O_{14}$ pyrochlore and the time that the varistor ceramics spend in the liquid phase. Therefore, the average size of ZnO grain is increased. When the content of Yb_2O_3 is more than 0.2%, the majority of the added Yb_2O_3 is much more segregated at the multiple ZnO grain junctions than between two ZnO grains. With increasing Yb_2O_3 additive content, the Yb_2O_3 phase is more distributed at the multiple ZnO grain junctions and the Yb_2O_3 between two ZnO grains is more discontinuously distributed. The grain size of these samples is relatively uniform without generating abnormal grain growth. The average grain size is markedly decreased when the Yb_2O_3 additive content is increased. Consequently, Yb_2O_3 acts as an inhibitor of grain growth [25].

The *E*−*J* characteristics of ZnO−Bi_2O_3-based varistor ceramics doped with different contents of Yb_2O_3 sintered at 900, 950 and 1 000 °C for 2 h are shown in Fig. 3. It is known that the sharper the knee of the curves between the linear region and the breakdown field is. the better the nonlinear characteristics is. In other words, the threshold voltage V_T, the nonlinear coefficient α, and the leakage current I_L are determined by the *E*−*J* curves [7]. As can be seen from Fig. 3(a), the *E*−*J* curves show that the nonlinear properties increase in the order of P0A→P3A→P4A→P1A→P2A, and the threshold voltage increases in the order of P1A→P2A→P0A→P3A→P4A, and Fig. 3(b) and Fig. 3(c) show the same order.

The densities of ZnO−Bi_2O_3-based varistor ceramics doped with different contents of Yb_2O_3 sintered at 900, 950 and 1 000 °C for 2 h are shown in Fig. 4. The results show that the higher the sintering temperature is, the lower the density of the varistor ceramics is. In general, the varistor ceramics sintered at 900 °C has the maximum density. The densification that occurs during sintering is a main factor in the Bi_2O_3 vaporization, and the higher the sintering temperature is, the more the Bi_2O_3 volatilizes. It is significant that the samples doped with various contents of Yb_2O_3 sintered at 900 °C and 950 °C have higher densities in comparison with the Yb_2O_3-free sample. The ytterbium ions have a larger radius (0.086 nm) than the zinc ions (0.074 nm). Relative atomic mass of zinc (65.39) is less than that of ytterbium (173.04). Thus, initial addition of Yb_2O_3 affects the grain distribution and develops different phases in the ceramic matrix, thereby increasing the bulk density initially. Further increase of the Yb_2O_3 content may mainly contribute to the change in grain size and phase distribution. So, bulk density increases with the Yb_2O_3 content then decreases at the different temperatures. The decrease in bulk density of the varistor ceramics with higher Yb_2O_3 content may be due to the increase of intragranular porosity [6], which is related with the vaporization of Bi_2O_3 from the ZnO−Bi_2O_3-based varistor ceramics. And the vaporization of Bi_2O_3 would affect the liquid phase reaction time, which is affected by the doping with rare earth oxides.

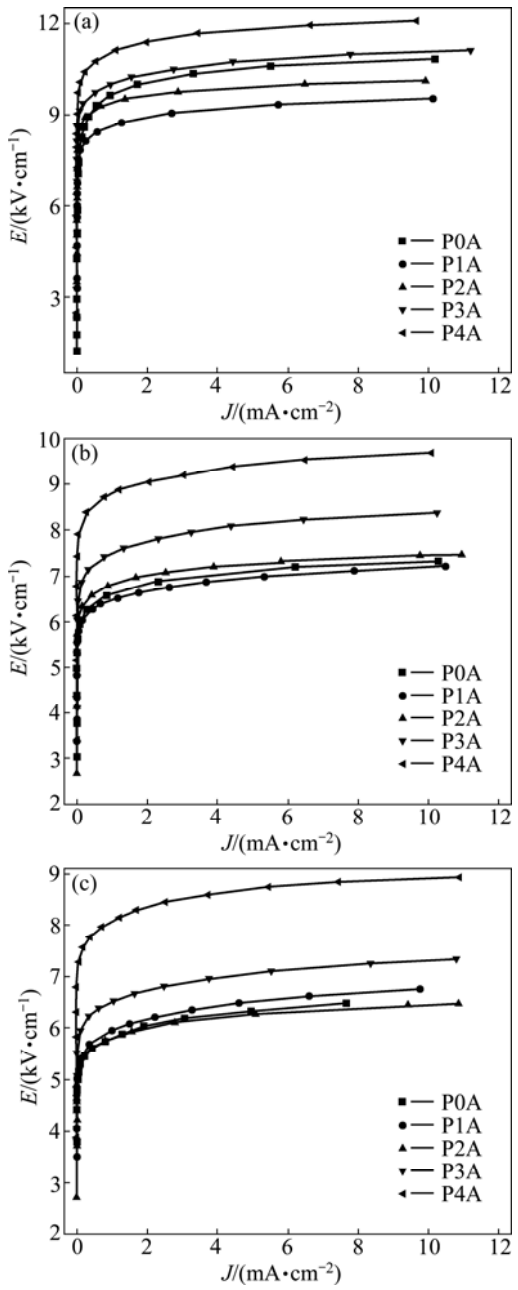

Fig. 3 *E*−*J* characteristics of ZnO−Bi_2O_3-based varistor ceramics doped with different contents of Yb_2O_3 sintered at different temperatures: (a) 900 °C; (b) 950 °C; (c) 1 000 °C

Figure 5 shows the variation of the threshold voltage (V_T) as a function of the content of Yb_2O_3 of ZnO−Bi_2O_3-based varistor ceramics sintered at different temperatures. With the variation of amount of rare earth

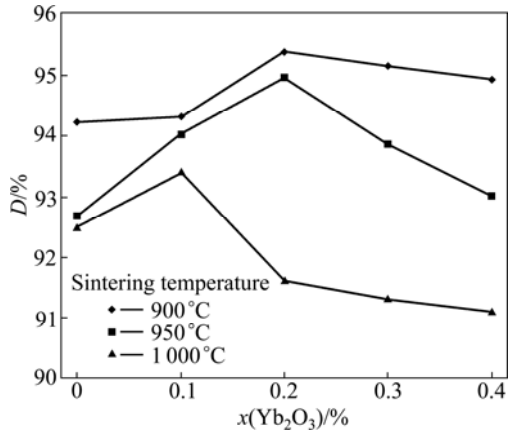

Fig. 4 Relative densities of ZnO−Bi_2O_3-based varistor ceramics doped with various contents of Yb_2O_3

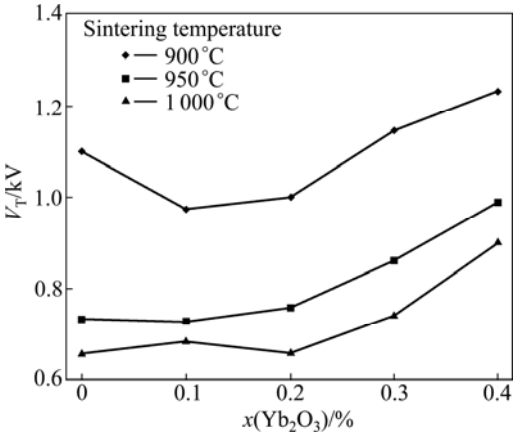

Fig. 5 Threshold voltage of ZnO−Bi_2O_3-based varistor ceramics doped with various contents of Yb_2O_3

and sintering temperature, the threshold voltage is between 656 V/mm and 1 232 V/mm. It is observed that the threshold voltage initially decreases and then increases with increasing the Yb_2O_3 content, and the similar changes of the threshold voltage at different sintering temperatures are found. The threshold voltage increases with the decrease of grains size. The higher the sintering temperature is, the lower the threshold voltage is, due to the grain growth at elevated temperatures. The maximum value of threshold voltage is found for 0.40% Yb_2O_3 doped varistor ceramics. Compared with the varistor ceramics without Yb_2O_3, the threshold voltages of varistor ceramics doped with 0.40% Yb_2O_3 are increased by 12%, 35% and 37% Yb_2O_3, respectively when sintered at three different temperatures.

Figure 6 shows the variation of the nonlinear coefficient (α) as a function of Yb_2O_3 content of ZnO−Bi_2O_3-based varistor ceramics sintered at 900, 950 and 1 000 °C for 2 h. With the variation of amount of rare earth and sintering temperature, the nonlinear coefficient is in the range of 14.1−22.3. It is seen that the nonlinear coefficient initially increases and then decreases with increase of the content of Yb_2O_3 basically.

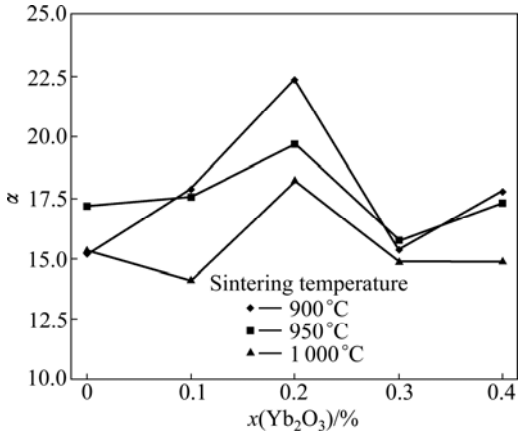

Fig. 6 Nonlinear coefficient of ZnO−Bi_2O_3-based varistor ceramics doped with different contents of Yb_2O_3

As a factor of characterizing nonlinearity of the varistor ceramics, the nonlinear coefficient varies from a maximum of 22.3 in 0.20% Yb_2O_3 doped ZnO−Bi_2O_3-based varistor ceramics sintered at 900 °C to a minimum of 14.1 in 0.10% Yb_2O_3 doped ZnO−Bi_2O_3-based varistor ceramics sintered at 1 000 °C. Yb_2O_3 is involved in the formation of interfacial states and deep bulk traps, and our previously research [13] indicated that the doping with rare earth oxides would affect the formation and decomposition of the $Bi_3Zn_2Sb_3O_{14}$ pyrochlore. Meanwhile, Yb_2O_3 would affect the time that the varistor ceramics spend in the liquid phase. As the time becomes longer, the vaporization of Bi_2O_3 from the ZnO–Bi_2O_3-based varistor ceramics becomes more serious, both of which contribute to the highly nonlinear properties [6]. It is seen that an increase of Yb_2O_3 content above 0.20% deteriorates the nonlinear properties.

Figure 7 shows the variation of the leakage current (I_L) as a function of Yb_2O_3 content of ZnO−Bi_2O_3-based varistor ceramics sintered at different temperatures. With the variation of amount of rare earth and sintering temperature, the leakage current is between 0.60 μA and 19.6 μA. There is no significant increase of leakage

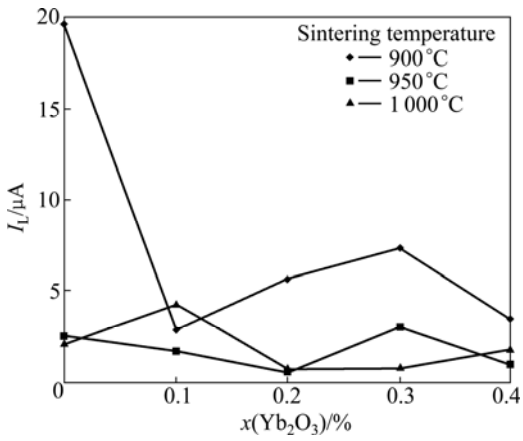

Fig. 7 Leakage current of ZnO−Bi_2O_3-based varistor ceramics doped with different contents of Yb_2O_3

current of ZnO−Bi_2O_3-based varistor ceramics doped with 0.10%−0.40% Yb_2O_3, and the leakage current is in the range of 0−8 μA. Moreover, the variation of the leakage current value is opposite to the nonlinear coefficient. This is because the high nonlinear coefficient leads to low leakage current due to relatively high tunneling current and the low nonlinear coefficient value leads to high leakage current due to relatively high thermionic emission current [7].

4 Conclusions

1) The addition of Yb_2O_3 results in the formation of the ZnO phase, Bi_2O_3 phase, $Zn_7Sb_2O_{12}$-type spinel phase and $Zn_2Bi_3Sb_3O_{14}$-type pyrochlore, and the Yb_2O_3 phases and Sb_2O_4 phase are found in ZnO−Bi_2O_3-based varistor ceramics with increasing contents of Yb_2O_3. The average size of ZnO grain is firstly increased and then decreased with the increase of Yb_2O_3 content.

2) The threshold voltage is between 656 V/mm and 1 232 V/mm, the nonlinear coefficient is in the range of 14.1−22.3, and the leakage current is between 0.60 μA and 19.6 μA. The ZnO−Bi_2O_3-based varistor ceramics with 0.20% (molar fraction) Yb_2O_3 sintered at 900 °C exhibits comparatively ideal comprehensive electrical properties with the threshold voltage of 999 V/mm, the nonlinear coefficient of 22.3 and the leakage current of 5.59 μA.

References

[1] LOOK D C. Recent advances in ZnO materials and devices [J]. Materials Science and Engineering B, 2001, 80(1/2/3): 383−387.

[2] HAN J P, SENOS A, MANTAS P Q. Varistor behaviour of Mn-doped ZnO ceramics [J]. Journal of the European Ceramic Society, 2002, 22(9/10): 1653−1660.

[3] CLARKE D R. Varistor ceramics [J]. Journal of the American Ceramic Society, 1999, 82(3): 485−502.

[4] ASHRAF M A, BHUIYAN A H, HAKIM M A, HOSSAIN M T. Microstructure and electrical properties of Sm_2O_3 doped Bi_2O_3-based ZnO varistor ceramics [J]. Materials Science and Engineering B, 2011, 176(11): 855−860.

[5] HE Jin-liang, LIU Jun, HU Jun, LONG Wang-cheng. AC ageing characteristics of Y_2O_3-doped ZnO varistors with high voltage gradient [J]. Materials Letters, 2011, 65(17/18): 2595−2597.

[6] ASHRAF M A, BHUIYAN A H, HAKIM M A, HOSSAIN M T. Microstructure and electrical properties of Ho_2O_3 doped Bi_2O_3-based ZnO varistor ceramics [J]. Physica B: Condensed Matter, 2010, 405(17): 3770−3774.

[7] NAHM C, SHIN B, MIN B. Microstructure and electrical properties of Y_2O_3-doped ZnO-Pr_6O_{11}-based varistor ceramics [J]. Materials Chemistry and Physics, 2003, 82(1): 157−164.

[8] PENG Zhi-jian, FU Xiu-li, ZANG Yan-xu, FU Zhi-qiang, WANG Cheng-biao, QI Long-hao, MIAO He-zhuo. Influence of Fe_2O_3 doping on microstructural and electrical properties of ZnO-Pr_6O_{11} based varistor ceramic materials [J]. Journal of Alloys and Compounds, 2010, 508(2): 494−499.

[9] HOUABES M, METZ R. Rare earth oxides effects on both the threshold voltage and energy absorption capability of ZnO varistors [J]. Ceramics International, 2007, 33(7): 1191−1197.

[10] PARK J S, HAN Y H, CHOI K H. Effects of Y_2O_3 on the microstructure and electrical properties of Pr-ZnO varistors [J]. Journal of Materials Science: Materials in Electronics, 2005, 16(4): 215−219.

[11] NAHM C W. Electrical properties and stability of praseodymium oxide-based ZnO varistor ceramics doped with Er_2O_3 [J]. Journal of the European Ceramic Society, 2003, 23(8): 1345−1353.

[12] XU Dong, CHENG Xiao-nong, ZHAO Guo-ping, YANG Juan, SHI Li-yi. Microstructure and electrical properties of Sc_2O_3-doped ZnO-Bi_2O_3-based varistor ceramics [J]. Ceramics International, 2011, 37(3): 701−706.

[13] XU Dong, SHI Xiao-feng, CHENG Xiao-nong, YANG Juan, FAN Yue-e, YUAN Hong-ming, SHI Li-yi. Microstructure and electrical properties of Lu_2O_3-doped ZnO-Bi_2O_3-based varistor ceramics [J]. Transactions of Nonferrous Metals Society of China, 2010, 20(12): 2303−2308.

[14] XU Dong, CHENG Xiao-nong, YUAN Hong-ming, YANG Juan, LIN Yuan-hua. Microstructure and electrical properties of $Y(NO_3)_3{\cdot}6H_2O$-doped ZnO-Bi_2O_3-based varistor ceramics [J]. Journal of Alloys and Compounds, 2011, 509(38): 9312−9317.

[15] XU Dong, SHI Li-yi, WU Zhen-hong, ZHONG Qing-dong, WU Xin-xin. Microstructure and electrical properties of ZnO-Bi_2O_3-based varistor ceramics by different sintering processes [J]. Journal of the European Ceramic Society, 2009, 29(9): 1789−1794.

[16] XU Dong, CHENG Xiao-nong, YAN Xue-hua, XU Hong-xing, SHI Li-yi. Sintering process as relevant parameter for Bi_2O_3 vaporization from ZnO-Bi_2O_3-based varistor ceramics [J]. Transactions of Nonferrous Metals Society of China, 2009, 19(6): 1526−1532.

[17] WU Zhen-hong, FANG Jian-hui, XU Dong, ZHONG Qing-dong, SHI Li-yi. Effect of SiO_2 addition on the microstructure and electrical properties of ZnO-based varistors [J]. International Journal of Minerals, Metallurgy and Materials, 2010, 17(1): 86−91.

[18] XU Dong, ZHANG Chen, CHENG Xiao-nong, FAN Yue-e, YANG Tao, YUAN Hong-ming. Dielectric properties of Zn-doped CCTO ceramics by sol-gel method [J]. Advanced Materials Research, 2011, 197/198: 302−305.

[19] METZ R, DELALU H, VIGNALOU J R, ACHARD N, ELKHATIB M. Electrical properties of varistors in relation to their true bismuth composition after sintering [J]. Materials Chemistry and Physics, 2000, 63(2): 157−162.

[20] LEITE E R, NOBRE M A, LONGO E, VARELA J A. Microstructural development of ZnO varistor during reactive liquid phase sintering [J]. Journal of Materials Science, 1996, 31(20): 5391−5398.

[21] LAO Y W, KUO S T, TUAN W H. Effect of Bi_2O_3 and Sb_2O_3 on the grain size distribution of ZnO [J]. Journal of Electroceramics, 2007, 19(2/3): 187−194.

[22] BERNIK S, MACEK S, AI B. Microstructural and electrical characteristics of Y_2O_3-doped ZnO-Bi_2O_3-based varistor ceramics [J]. Journal of the European Ceramic Society, 2001, 21(10/11): 1875−1878.

[23] XU Dong, CHENG Xiao-nong, WANG Ming-song, SHI Li-yi. Microstructure and electrical properties of La_2O_3-doped ZnO-Bi_2O_3-based varistor ceramics [J]. Advanced Materials Research, 2009, 79/80/81/82: 2007−2010.

[24] NAHM C W, PARK C H. Effect of Er_2O_3 addition on the microstructure, electrical properties, and stability of Pr_6O_{11}-based ZnO ceramic varistors [J]. Journal of Materials Science, 2001, 36(7): 1671−1679.

[25] NAHM C W, PARK C H. Microstructure, electrical properties, and degradation behavior of praseodymium oxides-based zinc oxide varistors doped with Y_2O_3 [J]. Journal of Materials Science, 2000, 35(12): 3037−3042.

(Edited by HE Yun-bin)